

# High-precision method for determining the position of laser beam focal plane\*

Ya.I. Malashko, A.N. Kleimenov, I.B. Potemkin, V.M. Khabibulin

**Abstract.** The method of wavefront doubled-frequency spherical modulation for determining the laser beam waist position has been simulated and experimentally studied. The error in determining the focal plane position is less than  $10^{-5} D$ . The amplitude of the control doubled-frequency electric signal is experimentally found to correspond to 12% of the total radiation power.

**Keywords:** laser beam, focusing, adaptive optics, wavefront doubled-frequency spherical probing.

## 1. Introduction

Spherical beam defocusing (especially under moving-base conditions) is an aberration with the largest amplitude, which increases most significantly the angular beam divergence. In this case, the spherical-probing signal in the modal control of adaptive system, which can be obtained by probing with respect to the wavefront spherical component when ‘approaching the vertex’ in the hill-climbing algorithm [1, 2], tends to zero (because the first derivative near the hill vertex tends to zero), and the adaptive system cannot reduce the error of the method. The reason is that the control signal is generated at the probing frequency. At the same time, the double-frequency probing signal increases and reaches a maximum value on the hill vertex. Therefore, a high-precision method of searching for the focal plane position can be developed using a wavefront double-frequency spherical probing signal.

In this paper, we report the results of numerical simulation and experimental determination of some parameters of wavefront double-frequency spherical modulation [3, 4], such as the error in determining the laser-beam waist position, radiation power conversion efficiency into a double-frequency signal, and some other characteristics.

This method is based on the fact that, only near the focal plane and only in the paraxial part of the beam waist, the power density changes upon wavefront double-frequency spherical modulation. It can be seen in Fig. 1 that the signal on the detector behind the diaphragm passes twice through the maximum during one period of wavefront spherical modulation; this fact indicates generation of a double-frequency signal.

\* Reported at the ‘Laser Optics’ Conference (St. Petersburg, Russia, June 2012).

Ya.I. Malashko, A.N. Kleimenov, I.B. Potemkin, V.M. Khabibulin  
JSC Concern ‘Almaz-Antey’, Leningradskii prosp. 80, 125190 Moscow,  
Russia; e-mail: malashko@yandex.ru, kleimenovandrei@rambler.ru

Received 24 October 2012; revision received 15 October 2013  
Kvantovaya Elektronika 43 (12) 1159–1164 (2013)  
Translated by Yu.P. Sin’kov

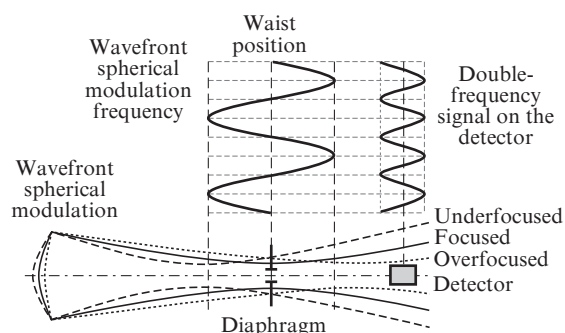


**Figure 1.** Schematic of the method for determining the position of the laser beam waist using a double-frequency wavefront spherical modulation signal.

Our study was aimed at solving the following problems:

- (i) search for a wavefront spherical modulation amplitude providing a maximum double-frequency signal;
- (ii) determination of the optimal diaphragm size corresponding to the maximum double-frequency signal;
- (iii) establishment of the range of focal plane displacements with respect to the observation plane which contains a double-frequency signal;
- (iv) determination of the relative fraction of the radiation power converted into the double-frequency signal;
- (v) analysis of the error of the method.

## 2. Results of numerical simulation of the double-frequency method

A laser beam of non-diffraction quality was modelled by the so-called Gaussian-like beam, the angular intensity distribution  $I(\varphi)$  in which is given by the expression

$$I(\varphi) = \frac{P_0}{2\pi\sigma^2} \exp\left(-\frac{\varphi^2}{2\sigma^2}\right), \quad (1)$$

where  $P_0$  is the total radiation power and  $\sigma$  is the standard deviation of the local wavefront angles of inclination that exceeds the diffraction limit.

A mathematical model was developed for a part of the experimental setup, which included a collimator of the OSK-2 objective (aperture 120 mm, focal length  $f = 1600$  mm), a flexible controlled bimorph mirror with a control zone diameter of 120 mm, a diaphragm, and a detector. A schematic diagram for multipath calculations is shown in Fig. 2. The model of Gaussian-like beam of non-diffraction quality used  $\sim 10^7$  rays uniformly distributed over the beam cross section at square-

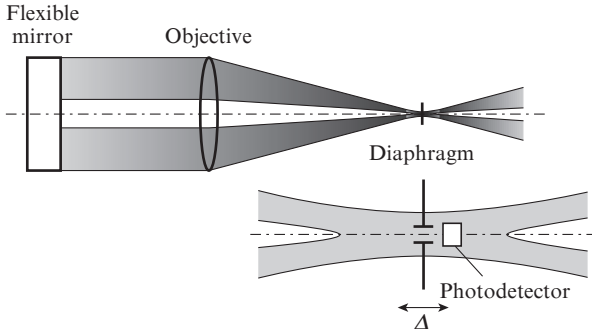


**Figure 2.** Schematic for simulating the parameters of the double-frequency method.

grid nodes. The angular distribution of local wavefront inclinations (rays) was set by a random-number generator according to the normal law with  $\sigma = \varphi_0/2.36$  ( $\varphi_0 = 40''$ ).

The numerical simulation revealed the laser-beam size in far-field zone to be

$$D = 2a/\varphi, \tag{2}$$

where  $a$  is the emitting aperture diameter. At distances exceeding (2) the beam angular distribution width changes by less than 1%–2%.

The calculated angular intensity distribution in the focal plane for a diaphragm displaced from the focus by  $\Delta$  is shown in Fig. 3. It can be seen that the intensity on the beam axis decreases to 0.8 of the maximum value at  $\Delta = -3.22$  and  $+3.63$  mm. Thus, the simulation results suggest the following formula for estimating the length of the ellipsoidal region where a double-frequency signal is generated at a level of 0.8 of the beam-axis intensity:

$$l = 2|\Delta| \approx 2 \times 0.9 \frac{f^2}{a} \varphi_0. \tag{3}$$

Below, we report the results of our experimental confirmation. Note that the waist length for a diffraction-limited beam is determined by the expression [5]

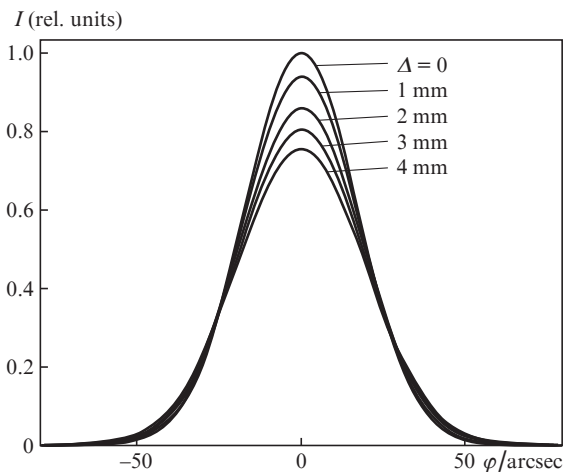


**Figure 3.** Normalised angular intensity distribution in the beam cross section at detector displacements by  $\Delta$  from the focus.

$$I_{\text{dif}} = 2|\Delta_{\text{dif}}| \approx 2 \times 0.5 \frac{f^2}{a} \frac{\lambda}{a}, \tag{4}$$

where  $\lambda$  is the radiation wavelength. With allowance for the fact that the diffraction divergence of a Gaussian beam of diameter  $a$  with a plane wavefront is  $1.22\lambda/a$ , the coefficients in formulas (3) and (4) differ by a factor of about 2.

Figure 4 shows the normalised angular intensity distribution in the objective focal plane when a spherical wavefront component with an amplitude  $2h$  is introduced by a flexible bimorph mirror. Figure 5 shows the calculated shapes of double-frequency signal at different modulation amplitudes provided by the flexible mirror and displacement  $\Delta = 0$ . It can

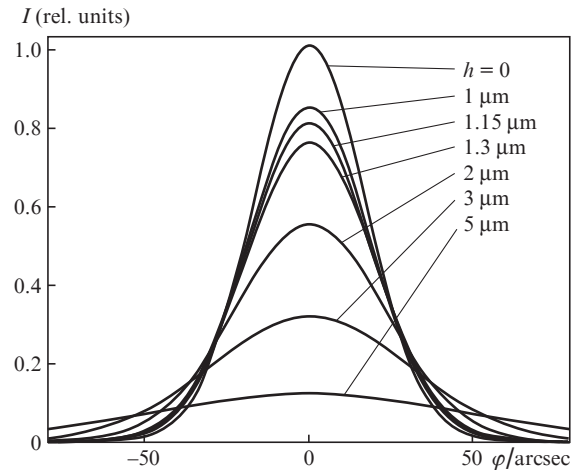


**Figure 4.** Normalised angular intensity distribution in the collimator focal plane at different flexible-mirror deformation amplitudes  $h$ . The focal plane displacements are  $\sim 2.842$ ,  $3.694$ , and  $5.697$  mm at  $h = 1.0$ ,  $1.3$ , and  $2.0$   $\mu\text{m}$ , respectively.

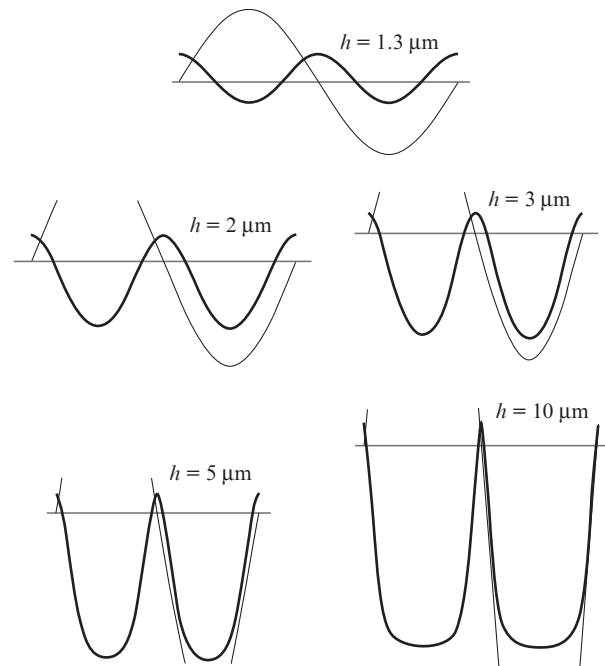


**Figure 5.** Shapes of the double-frequency signal at different flexible-mirror deformation amplitudes  $h$  (bold curves) and initial-signal shapes (thin curves).

be seen that a large modulation amplitude gives rise to a non-linear distortion, and the double-frequency signal becomes nonsinusoidal. Figure 6 shows the shapes and magnitude of double-frequency signal at different displacements  $\Delta$  of the focal plane from the diaphragm plane and an amplitude  $h = 1.3 \mu\text{m}$ .

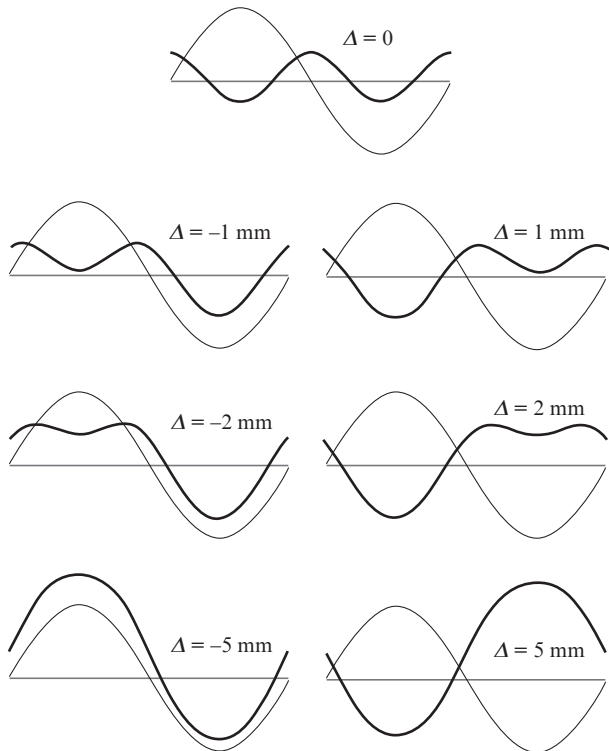


**Figure 6.** Shapes and magnitudes of the double-frequency signal at different displacements  $\Delta$  of the focal plane from the diaphragm plane (bold curves) and the initial-signal shapes (thin curves).

The model ‘oscillograms’ presented above indicate the following:

(1) The amplitude of a double-frequency signal without nonlinear distortions is maximum at the amplitude  $h = 1.3 \mu\text{m}$ , which corresponds to a waist longitudinal size of 3.2 mm (at an intensity level of 0.8 on the beam axis).

(2) The maximum fraction of the radiation power converted into a double-frequency signal is 11.5%.

Let us now discuss the way for choosing correctly the angular size  $\Delta\Omega$  of the diaphragm (Fig. 7) for the angular intensity distribution  $I_1(\varphi)$ . When a spherical aberration is introduced into the wavefront, the angular distribution  $I_2(\varphi)$  becomes wider and its amplitude at the center decreases (Fig. 7). The angular spacing between the intersection points of the curves  $I_1(\varphi)$  and  $I_2(\varphi)$  separates the central angular region of the initial beam (where power decreases) from the external region (in which, vice versa, an equivalent increase in power occurs). The simulation results show that the double-frequency signal is maximum when the intensity on the beam axis decreases to a level of 0.8. The curves  $I_1(\varphi)$  and  $I_2(\varphi)$  intersect at a level of 0.33 of the initial maximum  $I_1(\varphi)$ . The angular spacing between the intersection points exceeds the angular divergence by a factor of 1.3. However, according to the mathematical model, the maximum angular size of the diaphragm providing a maximum power should be equal to the angular FWHM of the initial Gaussian  $I_1(\varphi)$ , i.e., to the

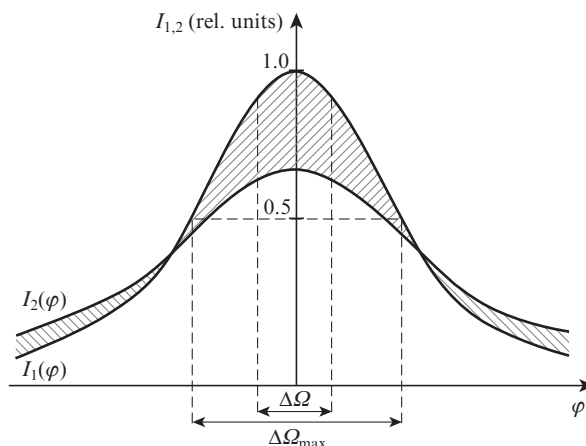


**Figure 7.** Exact choice of the angular size  $\Delta\Omega$  of the detector diaphragm. The  $\Delta\Omega_{\text{max}}$  value corresponds to the angular FWHM of the distribution  $I_1(\varphi)$ .

beam angular divergence  $\varphi_0$ . In our case [ $\varphi_0 = 40''$  (0.19 mrad) and  $f = 1600 \text{ mm}$ ], the calculated diaphragm diameter ( $d = f\varphi_0$ ) within which a double-frequency signal with maximum power is generated amounts to  $\sim 0.3 \text{ mm}$ . The difference in the volumes (the hatched area in Fig. 7) between the curves  $I_1(\varphi)$  and  $I_2(\varphi)$  with the angular widths  $\varphi_0$  and  $\Delta\Omega_{\text{max}}$  is insignificant (0.8%); therefore, it is difficult to find it experimentally.

### 3. Experimental

The schematic of the experimental setup for determining the error in finding the position of the laser beam waist is shown in Fig. 8. The radiation source is a single-mode GN-25 He-Ne

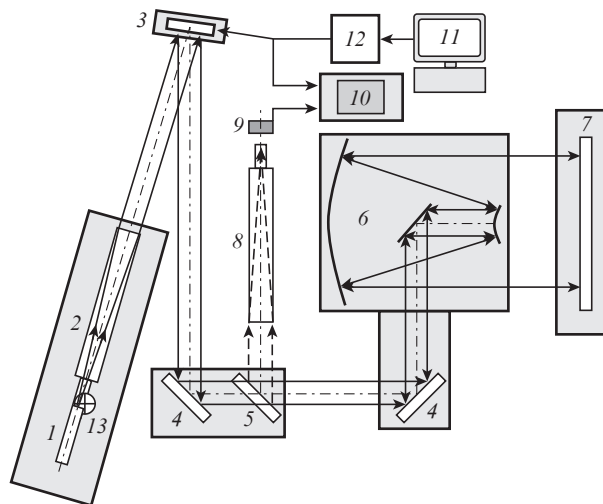


**Figure 8.** Schematic of the setup for finding the error in determining the laser beam waist position by wavefront double-frequency spherical probing:

(1) He-Ne laser ( $\lambda = 0.63 \mu\text{m}$ ,  $P_0 = 25 \text{ mW}$ ); (2) collimator 150 mm in diameter; (3) deformable bimorph mirror; (4) rotational reflector; (5) plane-parallel plate; (6) shaping telescope; (7) plane reference mirror 1 m in diameter; (8) receiving objective (diameter 150 mm,  $f = 1600 \text{ mm}$ ); (9) PD-24 K photodetector with a 0.3-mm diaphragm; (10) double-beam oscilloscope; (11) PC with a software for controlling the deformable mirror; (12) high-voltage amplifier; (13) modulator ( $\nu_{\text{mod}} = 230 \text{ Hz}$ ).

laser. The laser parameters are as follows: wavelength  $0.63 \mu\text{m}$ , output-beam diameter  $1.5 \text{ mm}$ , power  $25 \text{ mW}$ , and beam divergence  $1.2 \text{ mrad}$ . A laser beam, expanded by a collimator to a diameter of  $120 \text{ mm}$ , is incident on a controlled deformable mirror. The mirror is controlled via a personal computer using a special program. When identical voltages are applied to all drives, the mirror takes a spherical shape. The program works in an automatic frequency regime. We used a spherical modulation frequency of  $1 \text{ Hz}$  (note that the double-frequency effect is independent of the modulation frequency [3, 4]).

After reflection from the deformed mirror at an angle less than  $10^\circ$  (the wavefront distortion is two times larger), the laser beam is reflected from a plane rotation mirror and passes through the telescope formed. Then, being reflected from a plane reference mirror  $1 \text{ m}$  in diameter, the beam returns back to the telescope. The beam aperture at the telescope output is  $0.7 \text{ m}$ . Then the beam is directed by a receiving objective with a diameter of  $150 \text{ mm}$  and a focal length of  $1600 \text{ mm}$  to pass through a plane-parallel plate and fall on a photodetector based on a PD-24K photodiode with a  $0.3\text{-mm}$  diaphragm. Thus, we aligned the transmitting and receiving apertures and, using a plane mirror, excluded measurements in the far-field zone, which made it possible to simplify the experiment.

The photodetector was connected to one of the channels of the two-channel oscilloscope. A signal for controlling the mirror (to implement its spherical deformation) was applied to the second channel of the oscilloscope. As a result, one could simultaneously observe the signal for controlling the adaptive mirror (i.e., the wavefront spherical modulation signal at the frequency  $\nu$ ) and the signal from the photodetector at the frequency  $2\nu$  on the oscilloscope (Figs 9, 10).

The axial size of the region of generation of the double-frequency signal was measured at a longitudinal displacement of the secondary mirror of the transmitting–receiving telescope to complete disappearance of the double-frequency signal at different wavefront spherical modulation amplitudes (corre-

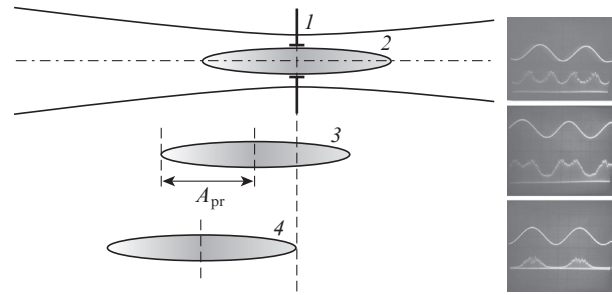


**Figure 9.** Middle positions of the waists in the region where frequency doubling may occur at a probing amplitude  $A_{pr}$  equal to the half waist length:

(1) diaphragm plane (reflecting surface), (2) symmetric (with respect to the diaphragm) position of the waist in the region of generation of maximum double-frequency signal, (3) displacement of the waist region where a double-frequency signal with distortions is generated, and (4) displacement of the waist region where the double-frequency signal is not observed; the corresponding oscillograms are on the right.

sponding to the mirror deformation amplitudes  $h = 1.1, 1.7, 2.3,$  and  $3 \mu\text{m}$ ). The amplitudes and shapes of the sinusoidal double-frequency signal and the spherical modulation signal were simultaneously observed on the oscilloscope (Fig. 10).

The axial displacement step of the secondary mirror was  $\Delta f = 50 \mu\text{m}$ , which corresponded to a change in the optical power by  $\Delta f/F^2 = 1.5 \times 10^{-5} \text{ D}$ . Here,  $F$  is the focal length of the main mirror of the transmitting–receiving telescope.

To determine the cross section of the region of generation of the double-frequency signal, we applied a set of calibrated diaphragms with sizes of  $0.1, 0.2, 0.3, 0.4,$  and  $0.5 \text{ mm}$ , placed in the collimator focal plane. The diaphragm with a diameter of  $0.3 \text{ mm}$  ( $40''$ ) was found to be optimal and consistent with the mathematical model under consideration.

The optical scheme contains a modulator (beam chopper), which allows one to record simultaneously the dc and ac com-

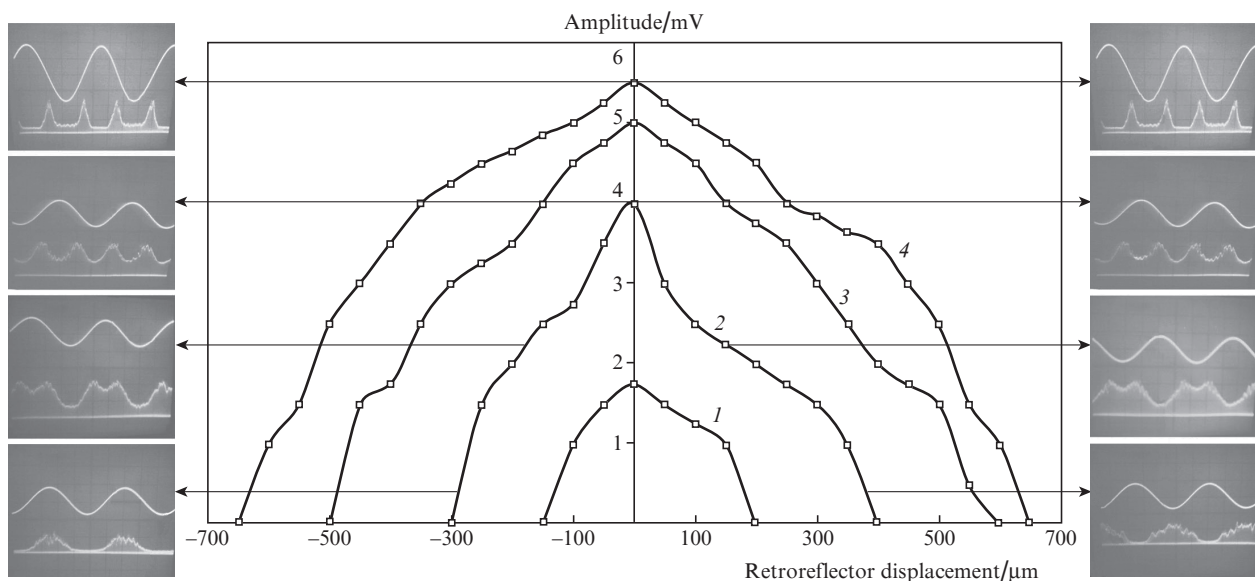


**Figure 10.** Dependences of the double-frequency signal amplitude on the retroreflector displacement at spherical modulation amplitudes  $h = (1) 1.1, (2) 1.7, (3) 2.3,$  and  $(4) 3 \mu\text{m}$ ; an output beam aperture of  $0.7 \text{ m}$ ; and a photodetector diaphragm diameter of  $0.3 \text{ mm}$ . The corresponding oscillograms are on the left and on the right.

ponents of the signal received by the photodetector for estimating the power transferred to the double-frequency signal; this approach allows one to reduce the error caused by the dc noise component. The frequency corresponding to 100% modulation of the radiation power was 230 Hz.

To find the fraction of the radiation power converted into the double-frequency signal, we recorded the dc component of the signal (under 100% modulation) received by the photodetector without a diaphragm and the amplitude of the ac component of the double-frequency signal recorded with an optimal diaphragm 0.3 mm in diameter (40").

#### 4. Experimental study of the region of generation of double-frequency signal

A stable undistorted double-frequency signal is observed in limited ranges of linear axial displacements of the retroreflector, mirror deformation amplitudes, and diaphragm sizes. The boundedness of the region of generation of the double-frequency signal ensures a high accuracy of the method.

A necessary condition for the formation of a double-frequency signal is the intersection of the waist volume by the diaphragm plane [Fig. 9, positions (2) and (3)]. When the waist center coincides with the diaphragm plane [Fig. 9, position (2)], the double-frequency signal is maximum and nonlinear distortions are absent. Under these conditions, the conversion efficiency of the radiation power into the double-frequency signal is maximum [Fig. 10, curve (2)]. The maximum signal is obtained at a diaphragm diameter of 0.3 mm, which is close to the angular beam divergence. At a mirror spherical probing amplitude of 1.7  $\mu\text{m}$ , the focal plane displacement was 3.2 mm, a value practically coinciding with the result of mathematical simulation.

In the case of large wavefront spherical modulation amplitudes [Fig. 10, curves (3), (4)], the double-frequency signal has a large amplitude, but nonlinear distortions are significant as well (see also Fig. 5).

The maximum in curve (2) in Fig. 10, which corresponds to undistorted double-frequency signal, was obtained under the following three conditions:

- (i) the waist midpoint lies in the diaphragm plane;
- (ii) the diaphragm diameter  $d \approx f\varphi_0$ ;
- (iii) the amplitude of waist displacement with respect to the diaphragm plane during wavefront spherical modulation amounts to half a waist length.

#### 5. Analysis of the error of the method

Figure 10 shows the results of recording the double-frequency signal amplitude for the optimal diaphragm 0.3 mm in diameter with a change in the spherical modulation amplitude by deformed mirror and with a displacement of the retroreflector of the telescope formed, which leads to the focus displacement. The curves cover the entire waist length, to complete disappearance of the double-frequency signal at both waist edges. The two upper curves are obtained at nonlinear distortions of the double-frequency sinusoidal signal. Nevertheless, the signal amplitude still increases, and the centres of these curves coincide well with those of the curves obtained without distortions.

It can be seen in Fig. 10 that the maxima of all curves are determined with an error smaller than a retroreflector displacement step (50  $\mu\text{m}$ ), which corresponds to a discrete change

in the optical power by  $1.5 \times 10^{-5} D$ . Thus, at any wavefront spherical modulation amplitudes, even in the case of nonlinear distortions, the error of the method analysed is less than  $10^{-5} D$ .

#### 6. Analysis of the double-frequency control signal amplitude

To estimate the fraction of the radiation power converted into a double-frequency signal, we chose a diaphragm 0.3 mm in diameter, a deformable-mirror spherical probing amplitude of 1.7  $\mu\text{m}$ , and the middle waist position (which coincides with the diaphragm plane). These conditions correspond to the complete use of the waist region, within which a double-frequency signal is formed; as a result, this signal attains a maximum without being nonlinearly distorted.

The relative fraction of the radiation power converted into the double-frequency signal was determined by measuring the total power and amplitude of the double-frequency signal. First, a cw He-Ne laser beam was directed to the photodetector and the beam power was modulated by a chopper at a frequency of 230 Hz (Fig. 11a). Then a 0.3-mm diaphragm was installed in front of the same detector (Fig. 11b). Finally, a deformable mirror with a spherical deformation amplitude of 1.7  $\mu\text{m}$ , which provides a double-frequency signal with a maximum amplitude, was added (Fig. 11c).

The oscillograms in Fig. 11 indicate that the double-frequency signal has an amplitude of 12%.

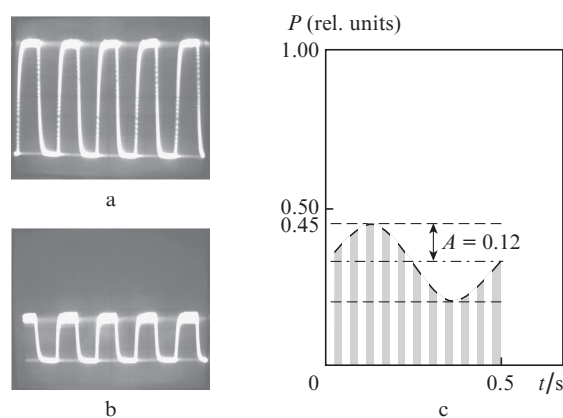


**Figure 11.** Technique for determining the relative fraction of the radiation power converted into a double-frequency signal from the oscillograms corresponding to beam interruption at a frequency of 230 Hz using a photodetector (a) without a diaphragm, (b) with a 0.3-mm diaphragm, and (c) with the same diaphragm and double-frequency signal modulation;  $A$  is the double-frequency signal amplitude.

#### 7. Conclusions

Based on the results obtained, we can conclude the following:

(1) The double-frequency method has a high spatial sensitivity, because a double-frequency signal is formed in a limited region adjacent to the beam waist plane.

(2) The double-frequency method can be used to determine the focal plane position with a high accuracy. For a beam aperture of 0.7 m and an angular beam divergence of 3.8", the error of this method is less than  $10^{-5} D$ .

(3) The radiation power converted into a double-frequency signal is independent of the modulation frequency.

(4) For an aperture of 0.7 m and an angular beam divergence of 3.8", it was experimentally found that the maximum amplitude of the double-frequency signal for controlling focusing corresponds to 12% of the total radiation power.

## References

1. Vitrichenko E.A. (Ed.) *Adaptivnaya optika* (Adaptive Optics) (Moscow: Mir, 1980).
2. Fried D.L. et al. *J. Opt. Soc. Am.*, **67**, 422 (1977).
3. Kleimenov A.N., Kochegarov Yu.M., Malashko Ya. I., Khabibulin V.M. In *Problemy sozdaniya lazernykh sistem* (Problems in Designing Laser Systems) (Raduzhnyi, 2008).
4. Kleimenov A.N., Malashko Ya.I., Potemkin I.B. *Naukoemkie Tekhnol.*, **12**, 85 (2011).
5. Born M., Wolf E. *Principles of Optics: Electromagnetic Theory of Propagation, Interference, and Diffraction of Light* (Oxford: Pergamon, 1964; Moscow: Nauka, 1973).